Journal of NAMP 72, (2026) 1-10

The Nigerian Association of Mathematical Physics

Journal homepage: https://nampjournals.org.ng

STUDY OF COMPOSITION OF BISMUTH OXIDE, CEMENT AND SAND AS X-RAY RADIATION SHIELDING MATERIALS

R.R. Dawam*[1], O. B. Sotanmide[1], B. Miri[1], F.B. Masok[2], B. O Rawen [3] S.A. Umar[4], A. M. Dunama[5]

[1]*Department of Physics, University of Jos, P.M B 2084 Jos, Plateau State, Nigeria.*
[2]*Department of Applied Physics, Plateau State University Bokkos, P.M.B, 2012, Jos, Plateau state, Nigeria.*
[3]*Directorate of Basic and Remedial Studies, Abubakar Tafawa Balewa University Bauchi, Bauchi, Nigeria*
[4]*Department of Physics, Faculty of Sciences, Federal University of Lafia, P. M. B 146, Lafia, Nasarawa State, Nigeria*
[5]*Muhammadu Buhari TETFund Centre for Excellence, Federal University of Lafia, P. M. B 146, Lafia, Nasarawa State, Nigeria*

ARTICLE INFO

Article history:
Received xxxxx
Revised xxxxx
Accepted xxxxx
Available online xxxxx

Keywords:
Bismuth oxide (Bi_2O_3), Radiation shielding, Cement, X-ray attenuation

ABSTRACT

*Composite samples of compositions (X-70) (SiO_2): X(Bi_2O_3): 30($3CaO.SiO_2$) were synthesized and studied for their ra*diation shielding properties. The density of each sample was measured using digital densimeter. The densities of the samples were found to increase as the quantity of bismuth oxide (Bi_2O_3) increases. The linear attenuation coefficient (LAC), mass attenuation coefficients (MAC), half value layer (HVL), tenth values layer (TVL), mean free path (MFP) of the samples were calculated from the experimental data. The results reveal that the values of LAC and MAC consistently decrease while the values of HVL, TVL and MFP increase steadily as the photon energy increases suggesting a good material for radiation shielding. The sample with 25 % of Bi_2O_3 suggested the most effective for radiation attenuation. This study highlights the possibility of locally obtained materials that are readily available and cost effective for viable radiation shielding applications as a worthwhile alternative to the conventional lead-based shielding materials.*

1. INTRODUCTION

X-ray radiation plays a crucial role in various scientific fields, including chemistry, materials science, medicine, and clinical settings. The high penetrating power of X-ray through dense materials enables the investigation of inner structures in both materials and the human body. It easing precise dose detection, flaw inspection, and radiation monitoring [1]. X-ray radiation has numerous applications such as imaging and is also use to enhances safety control in areas such as nuclear medicine [2]. However, excessive exposure to X-rays can lead to severe health risks, including radiation-related illnesses, injuries, and even death.

*Corresponding author: R.R. DAWAM
E-mail address: dawamr@unijos.edu.ng
https://doi.org/10.60787/jnamp.vol72no.656

To mitigate these risks, specially fabricated shielding materials needs to been developed to minimize exposure to X-ray radiation. Radiation shielding works by leveraging the interaction between radiation and materials, where the materials absorb or scatter the radiation, effectively reducing its intensity [3]. The ability of a shielding material to attenuate radiation depends on the density of the material and its atomic number [4]. Consequently, various materials have been explored for radiation shielding purposes, including clay-white cement mixtures, silica-based glasses, ball clay, kaolin-coated textiles, cement-based mortars with sand and eggshells as well as polymer nanocomposites [5-10].

Materials like lead, concrete, and aluminium are frequently used for radiation shielding, having been assessed for their ability to effectively block gamma rays and X-rays [3]. The lead-based shielding materials are commonly used due to their high shielding performance against X-rays [3]. However, the toxicity of lead poses a substantial concern, and its disposal after used can lead to environmental hazards [11] hence the need for a practical alternative.

Bismuth-based composites may standout in radiation shielding due to their exceptional attenuation properties [8]. By integrating bismuth with cement, shielding effectiveness may be greatly improved, which can present a potential replacement for conventional lead-based shielding materials. In spite of progress in radiation shielding materials, optimizing them for specific uses and as suitable substitute for lead, especially in extreme conditions, remains a challenge. Therefore, continuous research is crucial in other to create solutions that balance performance, cost, and environmental suitability. In addition to cost, the toxicity of lead presents a serious environmental and health risks, highlighting the need for safer, innovative and non-toxic alternatives that can provide reliable and versatile radiation protection while ensuring safety and practicality.

This study aimed to investigates X-ray attenuation performance of bismuth oxide (Bi_2O_3), silica (SiO_2), and cement ($3CaO.SiO_2$) embedded as a matrix with focus on material composition and energy dependence.

2 MATERIALS AND METHODS

2.1 Materials

The materials used in this study was bismuth which was collected from Abuja in Nigeria. The Bismuth was then taken to National Metallurgical Development Centre (NMDC) in Jos for separation of impurities that may be present. Bismuth was crushed into smaller particles and then grounded into powdered form. Other materials are cement ($3CaO.SiO_2$) and silica (SiO_2) which are commercially available in an open market in Jos, Plateau State. Figure 1 (a) shows the bismuth in clay form and Figure 1(b) illustrations the bismuth in its powdered form.

(a) Bismuth Clay

(b) Bismuth in powdered form

Figure 1

2.2. Sample preparation

The sample of bismuth oxide (Bi_2O_3) was in powdered form and was prepared for fabrication of the concrete according to the chemical formula ($(70-X)(SiO_2): X(Bi_2O_3):30(3CaO.SiO_2)$, where x = 5, 10, 15, 20 and 25 wt% by adding the percentage of Bi_2O_3, $3CaO.SiO_2$ and SiO_2. The mixture was properly done until a homogeneous solution was obtained. The mixture was then moulded in the fabricated mould of thickness 2.0 cm. Table 1 shows the compositions percentage of Bi_2O_3, SiO_2 and $3CaO.SiO_2$.

Table 1: Compositions of Fabricated Samples

Sample	Cement ($3CaO.SiO_2$)		Silica (SiO_2)		Bismuth oxide(Bi_2O_3)		Total composition	
X	%	mass(g)	%	mass(g)	%	mass(g)	%	mass(g)
5	30	21	65	45.5	5	3.5	100	70
10	30	21	60	42.0	10	7.0	100	70
15	30	21	55	38.5	15	10.5	100	70
20	30	21	50	35.0	20	14.0	100	70
25	30	21	45	31.5	25	17.5	100	70

2.3. Density of the samples

The densities of the samples were measuered using digital densimeter with model number MH-300A with an accuracy ±0.001 g/cm^3 using Archimedes' principle [12]. Table 2 shows the variation of densities with mass composition of Bi_2O_3, SiO_2 and $3CaO.SiO_2$. The densities of the samples increasing with increases in the composition of Bi_2O_3. Perhaps one can clearly said that density of the samples increases as the concentration of Bi_2O_3 increases with the composition of ($(70-X)(SiO_2): X(Bi_2O_3):30(3CaO.SiO_2)$).

Table 2. The density of the prepared samples in a concret form.

Sample wt%	Density (g/cm^3)
5.00	2.53
10.00	2.63
15.00	2.72
20.00	2.76
25.00	2.78

2.4 Radiation measurements

The setup of the experiment was discussed elsewhere by Masok et al [13]. X-ray attenuation efficiency experiments was carried out using Siemens Mobile X-ray machine (Serial No: 02441502). The tube voltage is in (kVp) and current in (mAs). The experiment was carried out at the voltage of 40 - 80 in step of 5 kVp and the current was constant at 20 mAs. The dose rates (in $\mu Sv/hr$) were recorded using a dosimeter GCA-07nW (Serial No: 10325) which is a digital Geiger counter with a Neon halogen tube and 0.38-inch mica window. The distance of separations between the point source and the detector was maintained at 100 cm throughout the experiment. The radiation attenuations testing was done by taking readings of different energies. Background readings were also recorded before the samples were placed in its holder for each of the chosen tube voltage/current.

RESULTS AND DISCUSSION

3.1 Linear attenuation coefficient (LAC) and Mass attenuation coefficient (MAC)

Linear attenuation coefficeint is important in shielding parameter, when a particle interact either by scattereing or absorption of photon. The attenuation is usually establish by the Lambert- Beer law[14, 15] stated as

$$I = I_o e^{-\mu t} \tag{1}$$

where I is the attenuated intensity, I_o is the unattenuated intensity , μ (cm^{-1}) is linear attenuation coefficient and t is the thickness of the material. The log of Eq.(1) can be expressed as

$$\mu = \frac{1}{t} ln(I_o/I) \tag{2}$$

Eq.(2) was used to calculate the values of LAC for the samples.

Figure 2 show the graph of linear attenuation coefficeient against the photon energy in (kVp) of the X-ray machine. The samples have diferent percentage concentration of Bi_2O_3 ranging from 5 to 25wt %. As can be seen from the graphs, the photon energy increases the value of LAC decreases up to 60 kVp. This indicates that great energy photons are less effective for the offset per thickness. Samples that has high percentage of Bi_2O_3 (sample with 20 and 25 wt%) has highest values of LAC. This signifies that it's the most effective for radiation shielding material per thickness. However, sample with 5 wt% has the lowest values of LAC indicating the less effect for radiation shielding material per thickness. This observation was also reported by Kaewjaeng et al [16] using glass material. At lower photons energy, all the materials are effective for radiation shielding per unit thickness. This suggest that the suitable material for radiation shielding is sample with 25 wt% of Bi_2O_3.

Mass attenuation coefficient is the quantity that defines the interaction probability between the X-ray photons and the mass per unit area for certain material. The mass attenuation coeffient (MAC) can be evaluated as

$$\mu_m = \left(\frac{\mu}{\rho}\right) = \sum_i w_i \left(\frac{\mu}{\rho}\right) \tag{3}$$

where ρ is the density of the material and w_i is the weight fraction of the ith element constituent [17]. Figure 3 shows the variation of MAC with the photons energy in (kVp). The values of all the samples decreases with increase in photons energy of the X-ray. This shows that in elevation photon energy is a lesser amount of effective per unit mass of the material. The values for all the samples decreases to minimal at 60 kVp. Sample with 25 wt% of Bi_2O_3 has high values of MAC making it the most effective for radiation shielding. This may be due to high atomic number in the sample[18]. In disparity the sample with less percentage of Bi_2O_3 has lower values of MAC making it the less effective for radiation shielding. Therefore, we may say that the best material for radiation shielding is sample with 25 wt% of Bi_2O_3.

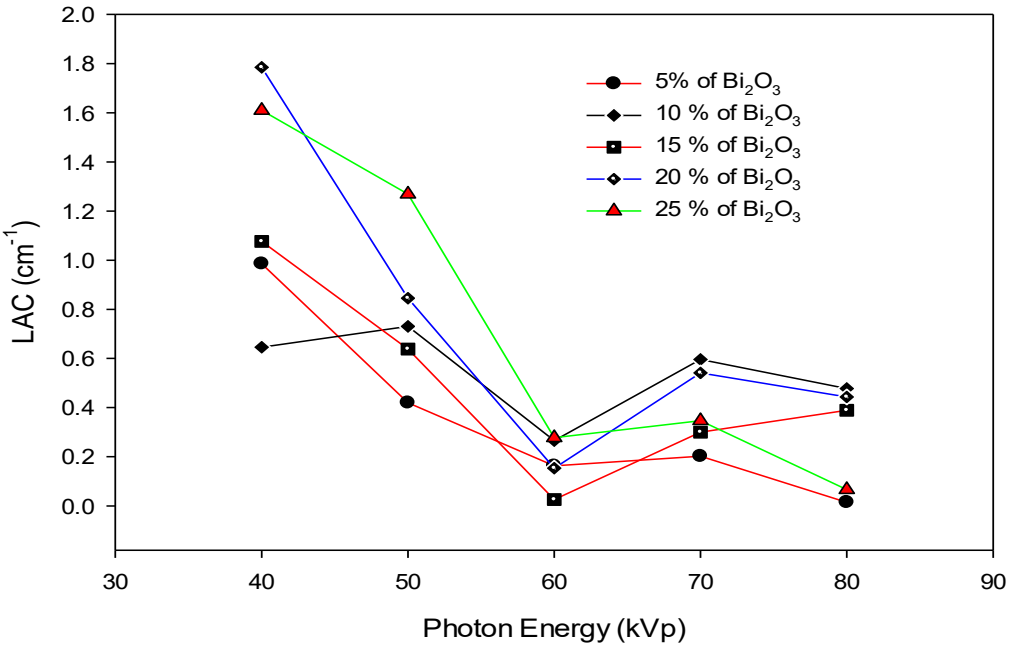

Figure 2. The variation of linear attenuation coefficient with photon energy for concentration of Bi_2O_3 from 5 to 25 wt%.

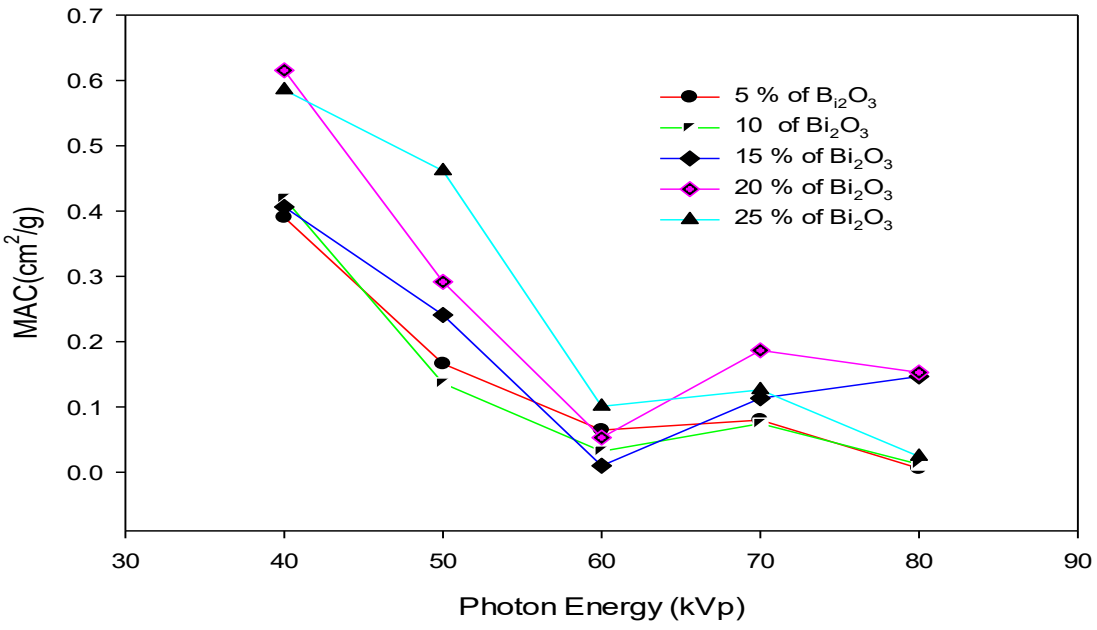

Figure 3. Variation of mass attenuation coefficient with photon energy for concentration of Bi_2O_3 from 5 to 25 wt%.

3.2 Half value layer (HVL), Tenth value layer (TVL) and Mean free path (MFP)

The HVL and TVL are necessary for thickness of the absorber material to decrease the radiation intensity by one half and one tenth respectively. The values of HVL and TVL were computed using Eq. (4) and (5) respectively [19, 20] as follows

$$\text{HVL} = \frac{In(2)}{\mu} \quad (4)$$

$$\text{TVL} = \frac{In(10)}{\mu} \quad (5).$$

However, the mean free path (MFP) is the average distance at which the photon travel through the sample without interaction. The MFP can be estimated [21] as

$$\text{MFP} = \frac{1}{\mu} \quad (6)$$

Figure 4 shows the graph of HVL as a function of photon energy for the samples of varying concentration from 5 to 25 wt% of Bi_2O_3. The plot illustrates that as photon energy increases the values of HVL also increases. It increases from the minimum value of 40kVp to 60 kVp and then decreases. This shows that high photon energy requires thicker material for radiation shielding. At lower energies, the variances in shielding efficiency are more noticeable, though at higher energies, the gap constricts as all materials struggle to attenuate high-energy photons.
Figure 5 illustrates the graph of TVL against photon energy. The values of photons energy also increase with TVL for all the samples. This specifies that high photon energy is necessary for denser materials.

Figure 6 shows graph of MFP as a function of photon energy in (kVp) for the samples of compositions $(70\text{-}X)(SiO_2)\text{: }X(Bi_2O_3)\text{:}30(3CaO.SiO_2)$, where x =5, 10, 15, 20 and 25 wt%. As the photon energy increases, the Mean Free Path (MFP) increases for all samples ranging from 5 to 25 wt%, signifying that higher-energy photons entail a more distance to interact with the material, making them more penetrating. This similar observation was reported [13].

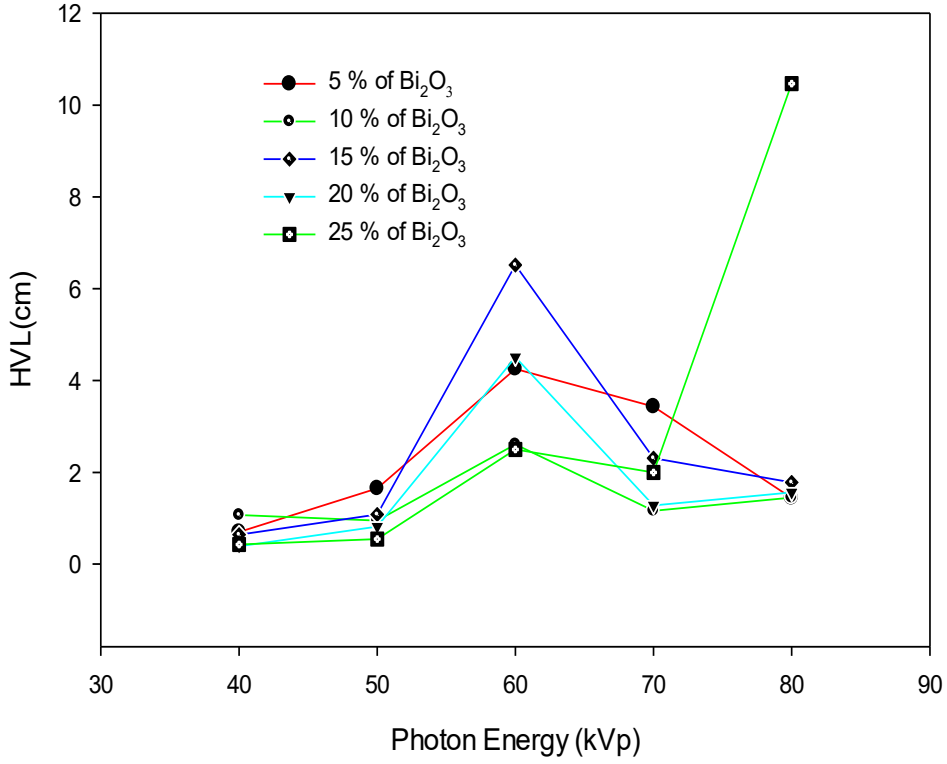

Figure 4. Plot of HVL against photon energy for samples.

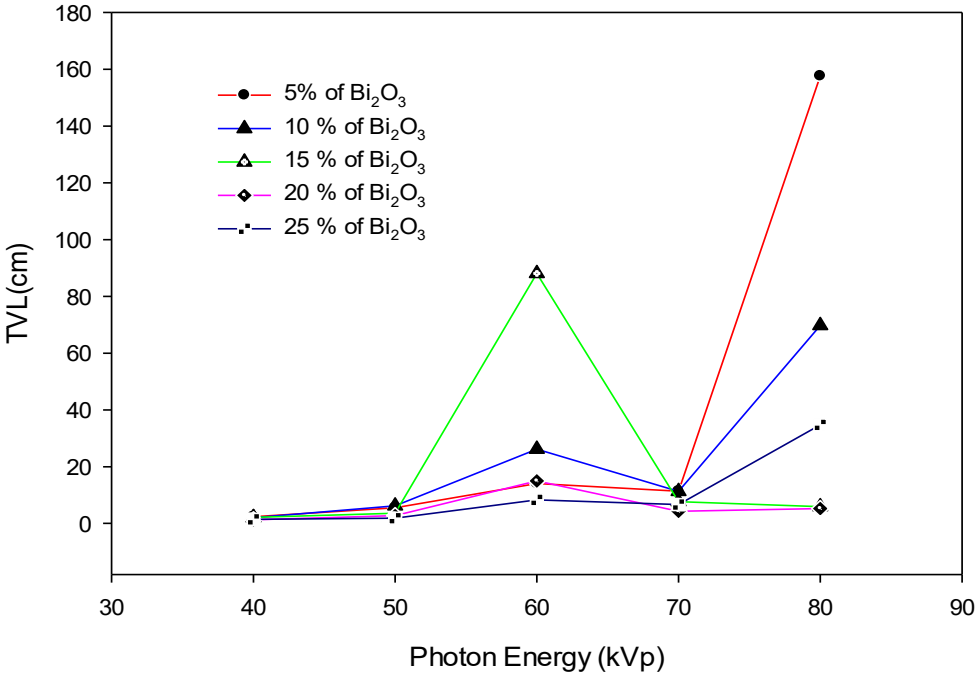

Figure 5. The graph of TVL as a function of photon energy for vary concentration of Bi_2O_3 between 5 to 25 wt%.

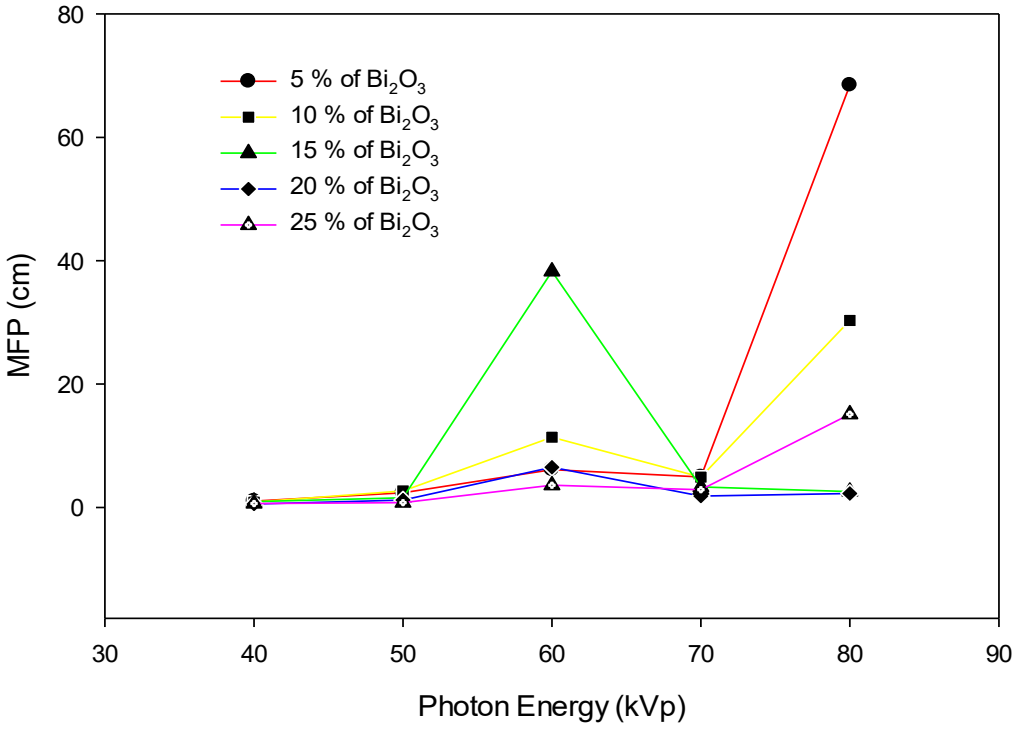

Figure 6. The plot of MFP against photon energy for samples with varying concentration between 5 to 25 wt% of Bi_2O_3.

CONCLUSION

The report presented on the study of composition of bismuth oxide, cement and sand as x-ray radiation shielding materials. The study provides a qualitative confirmation of X-ray attenuation principles. The samples were fabricated by using the chemical composition of (*70-X)(SiO_2): X(Bi_2O_3):30(3CaO.SiO_2)*, where X= 5, 10, 15, 20 and 25 wt%. The density of the samples wre determined using digital densimeter with model number MH-300A with an accuracy ±0.001 g/cm^3 by Archimedes' principle. It was observed that the density increases with increase in percentage composition of Bi_2O_3. The radiation attenuation shielding materials such as LAC, MAC, HVL, TVL and MFP were all evaluated. The results reveal that the composite composition of *Bi_2O_3, SiO_2* and *3CaO.SiO_2* can form a suitable radiation shielding material.

ACKNOWLEDGEMENTS

The work reported here was made possible by Muhammadu Buhari TETFund Centre for Excellence, Federal University of Lafia for allowing us to carried out the experiment in their Laboratory.

REFERENCES

[1] Lu, L., Peng, S., Zhao, L., Zhang, M., Xiao, J., Wen, H., & Xu, X. (2023). Visualized X- ray dosimetry for multienvironment applications. *Nano Letters*, *23*(18), 8753-8760.

[2] Zdora, M. C. (2021). X-ray Single-Grating Interferometry. In *X-ray Phase-Contrast Imaging Using Near-Field Speckles* (pp. 69-111). Cham: Springer International Publishing.

[3] Edmund, E., Amoako, J., Deatanyah, P., & Matulanya, M. (2024). Determination and Analysis of Radiation Shielding Properties of Some Selected Building Materials. *Radiation Science and Technology*, *10*(1), 11–20. https://doi.org/10.11648/j.rst.20241001.12.

[4] Naji, A. T., Jaafar, M. S., Ali, E. A., & Al-Ani, S. K. J. (2016). X-ray Attenuation and Reduction of Backscattered Radiation. *Applied Physics Research*, *8*(4), 92. https://doi.org/10.5539/apr.v8n4p92.

[5] Akbulut, S., Sehhatigdiri, A., Eroglu, H., & Celik, S. (2015). A research on the radiation shielding effects of clay, silica fume and cement samples. *Radiation Physics and Chemistry, 117, 88-92*.

[6] Aral, N., Nergis, F., & Candan, C. (2015). An alternative X-ray shielding material based on coated textiles. *Textile Research Journal, 86(7)*, 803-81.

[7] Binici, H., Aksogan, O., Sevinc, A. H., & Cinpolat, E. (2015). Mechanical and radioactivity shielding performances of mortars made with cement, sand and egg shells. *Construction and Building Materials, 93*, 1145-1150

[8] Nambiar, S., Osei, E. K., & Yeow, J. T. (2013). Polymer nanocomposite-based shielding against diagnostic X-rays. *Journal of Applied Polymer Science, 127(6)*, 4939.

[9] Olukotun, S. F., Gbenu, S. T., Ibitoye, F. I., Oladejo, O. F., Shittu, H. O., Fasasi, M. K., & Balogun, F. A. (2018). Investigation of gamma radiation shielding capability of two clay materials. *Nuclear Engineering and Technology, 50(6)*, 957-962

[10] Yasmin, S., Rozaila, Z. S., Khandaker, M. U., Barua, B. S., Chowdhury, F. U., Rashid, M. A., & Bradley, D. A. (2018). The radiation shielding offered by the commercial glass installed in Bangladeshi dwellings. *Radiation Effects and Defects in Solids, 173(7-8)*, 657-672.

[11] Moawad, E. M., Badawy, N. M., & Manawill, M. (2016). Environmental and occupational lead exposure among children in Cairo, Egypt: A community-based cross-sectional study. *Medicine, 95(36)*, 2976.

[12] M. K. Halimah, A. Azuraida, M. Ishak, and L. Hasnimulyati, "Influence of bismuth oxideon gamma radiation shielding properties of boro-tellurite glass," *J Non Cryst Solids*, vol. 512, 2019, doi:10.1016/j.jnoncrysol.2019.03.004.

[13] Masok, B. F., Aliyu, U. S. A., Dawam, R. R., Dunama, A. M., & Tolulope, O. S. (2025). X-Ray Shielding Characteristics of Sand Reenforced Plastic Concrete Blocks. *EDUCATUM Journal of Science, Mathematics and Technology*, *12*(1), 148-162.

[14] Issa, S. A., Rashad, M., Hanafy, T. A., & Saddeek, Y. B. (2020). Experimental investigations on elastic and radiation shielding parameters of WO3-B2O3-TeO2 glasses. *Journal of Non-Crystalline Solids*, *544*, 120207.

[15] Saudi, H. A., Tekin, H. O., Zakaly, H. M., Issa, S. A., Susoy, G., & Zhukovsky, M. J. O. M. (2021). The impact of samarium (III) oxide on structural, optical and radiation shielding properties of thallium-borate glasses: Experimental and numerical investigation. *Optical Materials*, *114*, 110948.

[16] S. Kaewjaeng, S. Kothan, N. Chanthima, H. J. Kim, and J. Kaewkhao, "Gamma radiation Shielding materials of lanthanum calcium silicoborate glasses," in *Materials Today: Proceedings*, Elsevier Ltd,2018, pp. 14901–14906. doi: 10.1016/j.matpr.2018.04.027.

[17] Jackson, D. F., & Hawkes, D. J. (1981). X-ray attenuation coefficients of elements and mixtures. *Physics Reports*, *70*(3), 169-233.

[18] Mhareb, M. H. A., Alqahtani, M., Alshahri, F., Alajerami, Y. S. M., Saleh, N., Alonizan, N., & Morsy, M. A. (2020). The impact of barium oxide on physical, structural, optical, and shielding features of sodium zinc borate glass. *Journal of Non-Crystalline Solids*, *541*, 120090.

[19] Husain, H. S., Rasheed Naji, N. A., & Mahmood, B. M. (2018). Investigation of Gamma Ray Shielding by Polymer Composites. *IOP Conference Series: Materials Science and Engineering*, *454*, 012131. https://doi.org/10.1088/1757-899X/454/1/012131.

[20] Şakar, E., Özpolat, Ö. F., Alım, B., Sayyed, M. I., & Kurudirek, M. (2020). Phy-X/PSD: development of a user friendly online software for calculation of parameters relevant to radiation shielding and dosimetry. *Radiation Physics and Chemistry*,1*66*, 108496.

[21] R. El-Mallawany and M. I. Sayyed, "Comparative shielding properties of some tellurite glasses: Part 1, *Physica B Condens Matter*, vol. 539, pp. 133–140, Jun. 2018, doi: 10.1016/j.physb.2017.05.021.